

# Fabrication and Characterization of Cypermethrin Nanocapsules in Miniemulsion Polymerization System

Chun-Miao Xia, Yi-Feng Zhou, Wang-Yan Nie, Lin-Yong Song, Ming-Dong Dai, Xiao-Ling Xu, Zhen Wang

AnHui Province Key Laboratory of Environment-friendly Polymer Materials,  
School of Chemistry and Chemical Engineering, Anhui University, Hefei 230039, China

Received 26 July 2011; Revised 7 November 2011; accepted 23 January 2012

DOI 10.1002/app.36866

Published online in Wiley Online Library (wileyonlinelibrary.com).

**ABSTRACT:** The nanoencapsulation of cypermethrin (CP) was carried out by miniemulsion polymerization, a convenient one-pot encapsulation technique for nanocapsules. The encapsulation was achieved by polymerization inducing phase separation within minidroplets dispersed in an aqueous phase. For nanocapsules prepared in this way, the type of surfactant and initiator, the level of the crosslinking agent or chain-transfer agent, and the monomer/CP ratio play a significant role in defining the end morphology of the latex particles. Specifically, for a styrene (St)/CP system, there

were optimum levels of ionic surfactant (1.0 wt % sodium dodecyl sulfate), nonionic surfactant [0.5 wt % poly(ethylene glycol) monoethylphenyl ether], oil-soluble initiator [1.0 wt % azobis(isobutyronitrile)], crosslinking agent (1.0 wt % divinylbenzene), and a St/CP ratio of 1 : 1 for obtaining well-defined nanocapsules of CP. © 2012 Wiley Periodicals, Inc. *J Appl Polym Sci* 000: 000–000, 2012

**Key words:** microencapsulation; morphology; phase separation

## INTRODUCTION

Nanocapsules are vesicular systems in which active substances are confined in a cavity consisting of an inner liquid surrounded by a polymeric membrane. One of their fundamental characteristics is their size, which is generally taken to be around 5–10 nm with an upper size limit of  $\sim 1000$  nm, although the range generally obtained is 100–500 nm. Polymer nanocapsules have been used for potential applications such as nanoreactors, dye dispersants, controlled-release of drugs (DDS), cosmetics, fillers, and catalysis.

A variety of nanocapsules have been prepared by different strategies, such as synthesis with solid templates,<sup>1–4</sup> layer-by-layer self-assembly based on electrostatic interaction,<sup>5–8</sup> and heterogeneous polymerization through the encapsulation of a liquid core.<sup>9–14</sup> The miniemulsion polymerization has been shown to be a promising technology because of its high efficiency and stability.

In general, miniemulsions consist of small, stable, and narrowly distributed droplets in a continuous phase. The system is obtained by high shear; for example, by ultrasonication or high-pressure homogenizers. The high stability of the droplets is ensured by the combination of the amphiphilic component, the surfactant, and the costabilizer, which is soluble and homogeneously distributed in the droplet phase.<sup>15</sup> In such a system, the hydrophobic cypermethrin (CP) is soluble in the monomer and can be used as a costabilizer. As such, one does not need a standard inert costabilizer, such as HD, which must be removed after polymerization in commercial applications.

CP is an effective pesticide against many pests, particularly Lepidoptera.<sup>16</sup> It has high-insecticidal potency and relatively low-side effects on birds and mammals, although it is acutely toxic to aquatic animals.<sup>17</sup> Here, we are interested in the special case of nanocapsules containing CP, which can result in sufficient effects on pests, yet reduce the side effects of the pesticide due to the small dosage used. Because of their small size, nanocapsules may be easy to deposit on the leaves of the plants, which helps to reduce waste of the pesticide. It is also a great advantage that pesticides encapsulated inside nanocapsules can be efficiently protected against enzymatic and hydrolytic degradation.

In this work, a miniemulsion polymerization is described that yields CP nanocapsules and consists

Correspondence to: Y.-F. Zhou (yifengzhou@126.com).

Contract grant sponsor: Scientific Research Fund of Anhui Provincial Education Department; contract grant number: KJ2009A51.

Contract grant sponsor: 211 Project of Anhui University.

**TABLE I**  
**Typical Mixture Compositions for the Synthesis of CP Nanocapsules**

Run	Water	SDS	OP-10	DNS-86	CP	St	AA	DVB	DDT	KPS	AIBN
1	80	0.1	0.2		3.3	10	0.2	0.2		0.2	
2	80	0.1	0.2		10	10	0.2	0.2		0.2	
3	80	0.1	0.2		10	10	0.2	0.2			0.2
4	80	0.1	0.2		10	10	0.2		0.06		0.2
5	80			0.3	10	10	0.2	0.2			0.2

The units used in this table are grams.

of a polymeric wall with a thickness in the nanometer region, filled with CP. To enable a stable dispersion, the capsule surface is stabilized by the adsorption of a combination of ionic and nonionic surfactants. The morphology of the demixing structure is determined by the type of the surfactant, initiator, the monomer/hydrocarbon ratio, and the level of the crosslinking agent or chain-transfer agent.

## EXPERIMENTAL

### Materials

Styrene (St), acrylic acid (AA), sodium dodecyl sulfate (SDS), poly(ethylene glycol) monoethylphenyl ether (OP-10), potassium persulfate (KPS), and azobis(isobutyronitrile) (AIBN) were provided by China National Pharmaceutical Group Corp. (Shanghai, China). The St and AA were distilled under reduced pressure for the removal of the inhibitor and stored in a refrigerator before use. The KPS was recrystallized twice from water. AIBN was recrystallized twice from anhydrous ethanol. Allyloxy polyoxyethylene (10) nonylammonium sulfate (DNS-86) was obtained from Shuangjian Co., Guangzhou, China. Divinylbenzene (DVB), supplied by Sigma-Aldrich, was a technical grade material containing 80 wt % of the divinyl monomer with the remaining 20 wt % being St and ethylstyrene. *N*-dodecanethiol (DDT) was supplied by Aladdin. CP was provided by Shanghai united Chemical Factory. DVB, DDT, and CP were used as received. Distilled water was used for all polymerizations and treatment processes.

### Synthesis of CP nanocapsules

The nanocapsules were elaborated through the encapsulation of CP in a miniemulsion polymerization. An aqueous solution of SDS, OP-10, or DNS-86 (stream A) and an oil mixture of St, AA, DVB or DDT, and CP (stream B) were mixed together. After pre-emulsification for 15 min by magnetic stirring, a homogenization process was carried out for another 15 min through high shear using a high-shear homogenizer (FM200, FLUKO, China) at 3000 r/min. The resulted miniemulsion was transferred into a three-necked round flask and stirred mechanically

with highly pure nitrogen bubbling for 30 min to remove any dissolved oxygen. An aqueous solution of KPS (stream C) was then injected into the system to start the polymerization. When AIBN was used, it had to be added to the monomer mixture before the water phase and oil phase were mixed, so that AIBN was evenly distributed in all the droplets formed. The reaction proceeded for 5 h under the protection of nitrogen at 75°C. The recipes for the synthesis of the nanocapsules are summarized in Table I.

### Characterization of the latex particles

The morphology of the latexes was observed by transmission electron microscopy (TEM; JEM, 2100, 200 kV, Japan). In a typical experiment, one drop of a diluted colloidal dispersion mixture was placed on a 200-mesh carbon-coated copper grid and was left to dry at room temperature before the observation.

The particle size and its distribution were measured by Particle Size Analyzer (Microtrac instrument, S3500, USA). Samples of latex particles were diluted with a 0.2 wt % aqueous solution of SDS before the measurement. Particle sizes are given as the average of three measurements.

<sup>1</sup>H NMR spectra were recorded on a Bruker-AV400 spectrometer using CDCl<sub>3</sub> as solvent.

Fourier transform infrared (FTIR) spectra were recorded using a Nicolet NEXUS-870 spectrometer on powder-pressed KBr pellets.

The thermal analyses of the nanocapsules and PSt were measured with a Q2000 differential scanning calorimeter (TA instruments). The sample was cooled to -80°C at 50°C min<sup>-1</sup> and maintained for 2 min and then scanned at a heating rate of 20°C min<sup>-1</sup> from -60°C to +140°C.

The drug-loading efficiency was measured on each batch. The latex product of the miniemulsion polymerization was demulsified by adding much ethanol. The polymer solid was collected by suction filtration and then purified to eliminate the adsorbed oligomers and unreacted monomer by washing it with water and then three times with ethanol. About 1.5 g dried polymer solid was packaged by filter paper and extracted for 10 h with acetone as solvent in

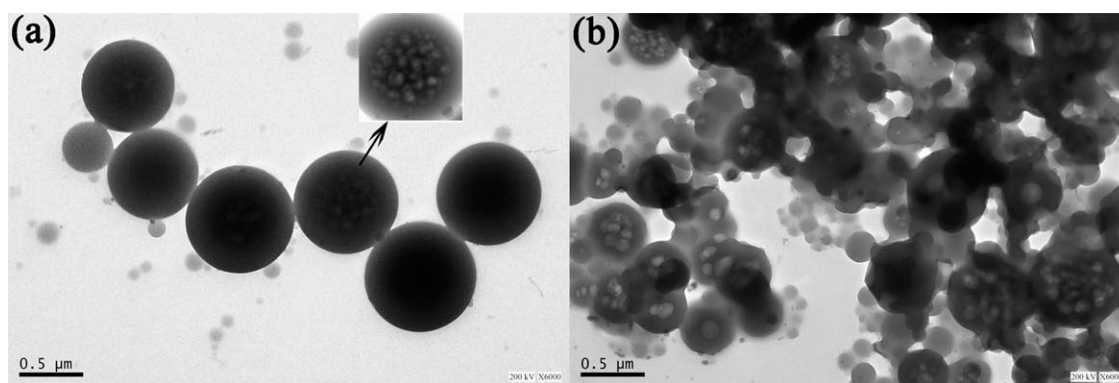


**Figure 1** TEM images of samples made with (a) 3 : 1 in Run 1 and (b) 1 : 1 St/CP ratios in Run 2.

a Soxhlet extractor. The package was then vaporized at room temperature and then dried under vacuum at 50°C until constant weight ( $W$ ). The drug-loading efficiency was calculated from the equation:

$$\text{Drug loading efficiency}(\%) = \frac{1.5 - W}{1.5} \times 100\%$$

## RESULTS AND DISCUSSION

As previously outlined, the successful formation of nanocapsules by phase separation in miniemulsion strongly depends on the reaction conditions. In the following, we explore the effects of some determining parameters (type of the surfactant, initiator, the monomer/CP ratio, and the level of the crosslinking agent or chain-transfer agent) on the creation of nanodroplets with emphasis on their morphologies.

In a miniemulsion polymerization, nanoencapsulation of a liquid substance is fulfilled through phase separation within the particles, which is triggered by the polymerization. The less water-soluble the hydrocarbon core (CP, in our case) and the higher the monomer content, the better the droplet stability. The difference of hydrophilicity between the hydrocarbon core and the polymer shell turned out to be the driving force for nanocapsule formation.<sup>18</sup> Monomer St is rather hydrophobic, and this created difficulties for the encapsulation of the hydrophobic CP. From a thermodynamic perspective, increasing the hydrophilicity of PSt chains should favor the encapsulation of CP. AA (1.0 wt %) is an effective concentration for assisting with the encapsulation of CP for the studied system.<sup>19</sup> For the following experiments, the level of added AA was set to 1.0 wt %.

### Influence of the variation of the St/CP ratio

The ratio of the shell polymer (PSt) to the CP (determined by the St/CP ratio in a recipe) has a great effect on the particle morphology and size. There-

fore, the influence of the ratio was investigated. TEM photographs of the resulting samples are shown in Figure 1. The white microdomains observed inside nanocapsules can be understandable considering that CP was vaporized during TEM measurement. When the amount of added CP is very low in Run 1, as shown in Figure 1(a), both nanocapsules and nanoparticles were produced by the polymerization of the miniemulsion droplets. Because of low fraction of CP, the microdomains are not discernible. As seen from Figure 2(a), the size distribution curve is bimodal. The average diameter of nanoparticles is around 183 nm, when nanocapsules' average diameter is around 605 nm. Two volume fractions of nanoparticles and nanocapsules are well separated in the size distribution spectrum, which is 44 and 56%, respectively. The undesirable nanoparticles were presumably formed by homogeneous nucleation because of larger monomer concentration in the oil phase.

In Figure 1(b), the number of nanocapsules, which is like porous structure, was found to increase largely upon increasing the amount of CP to 10 g in Run 2. This can also be clearly seen in the size distribution of all nanoparticles and nanocapsules. As shown in Figure 2(a,b), the volume fraction of nanocapsules linearly increased from 56 to 84% when the amount of CP was increased from 3.3 to 10 g. It turned out to be difficult to attain good capsules when the St/CP ratio was above 3 : 1. A large content of monomer in the oil phase is detrimental to the formation of nanocapsules.

### Influence of the initiator type

Another important parameter is the type of initiator that has a large influence on the particle morphology, because the formation of capsules is correlated with the locus of nucleation. Landfester and coworkers<sup>10</sup> reported that the use of a standard water-soluble ionic initiator, KPS, to start the polymerization however leads for polystyrene solid particles in

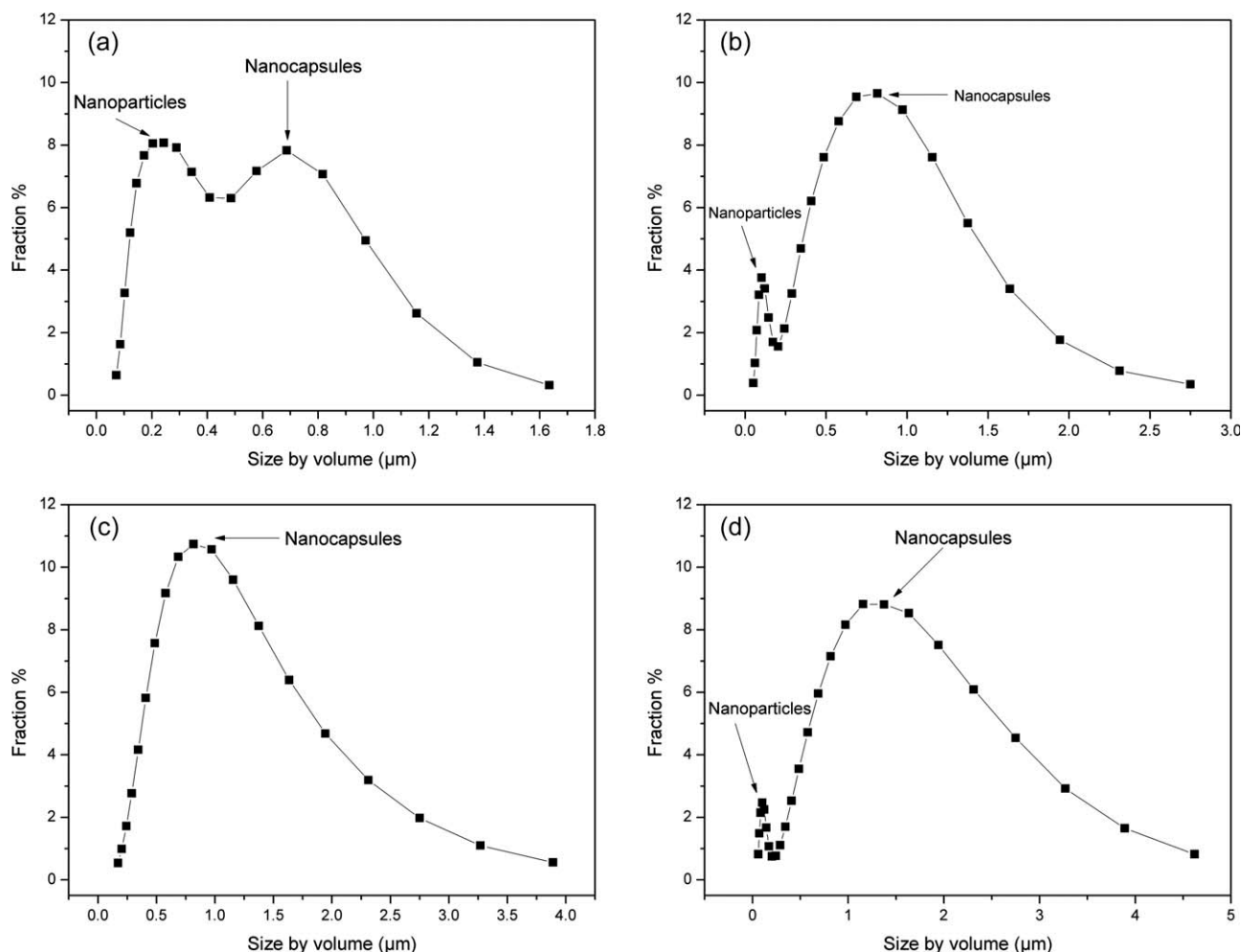


**Figure 2** Size distribution of all nanoparticles and nanocapsules of samples with different recipe: Run 1 (a), Run 2 (b), Run 3 (c), and Run 4 (d).

no case to the formation of nanocapsules. As for AIBN, the homogeneous nucleation is less likely.<sup>20</sup> According to this opinion, two miniemulsion polymerizations were carried out by, respectively, using KPS and AIBN as initiator, whose TEM images are shown in Figure 3. It was easy to gain nanocapsules under an oil initiator (AIBN) in Run 3, as shown in Figure 3(b,d), while a large fraction of oligomers and nanoparticles dotted around nanocapsules was inclined to be formed when water-soluble ionic initiator (KPS) in Run 2 was used, as shown in Figure 3(a,c). Under higher magnification, we can observe an obvious difference in the morphologies between the KPS- and AIBN-initiated systems in Figure 3(c,d). A nanocapsule coexists with a small fraction of pure PSt nanoparticles and many oligomers that are created by homogeneous nucleation as shown in Figure 3(c), while we can see a rather pretty nanocapsule without any oligomers dotted around as shown in Figure 3(d).

In the case of KPS-initiated system, the particle size distribution becomes pronouncedly bimodal:

nanoparticles with smaller size and nanocapsules with larger size, as shown in Figure 2(b). When AIBN is used, the particle size distribution becomes monomodal: most of particles were nanocapsules, as shown in Figure 2(c). It is inferred that the use of the hydrophobic initiator AIBN is advised, facilitating the encapsulation of CP in our case, otherwise secondary nucleation of pure PSt.

### Influence of the polymer mobility

The principle of encapsulation by miniemulsion polymerization is phase separation induced by polymerization. The polymer mobility plays a significant role in influencing the phase separation of particles. The mobility of polymer chains can be conveniently adjusted by adding crosslinkers or chain-transfer agent to the system. The influence was studied through the addition of a crosslinking agent DVB or chain-transfer agent DDT into the system. Nanocapsules dominate in the latex particles with the addition of 1 wt % DVB in Run 3 [Fig. 4(a,c)], while



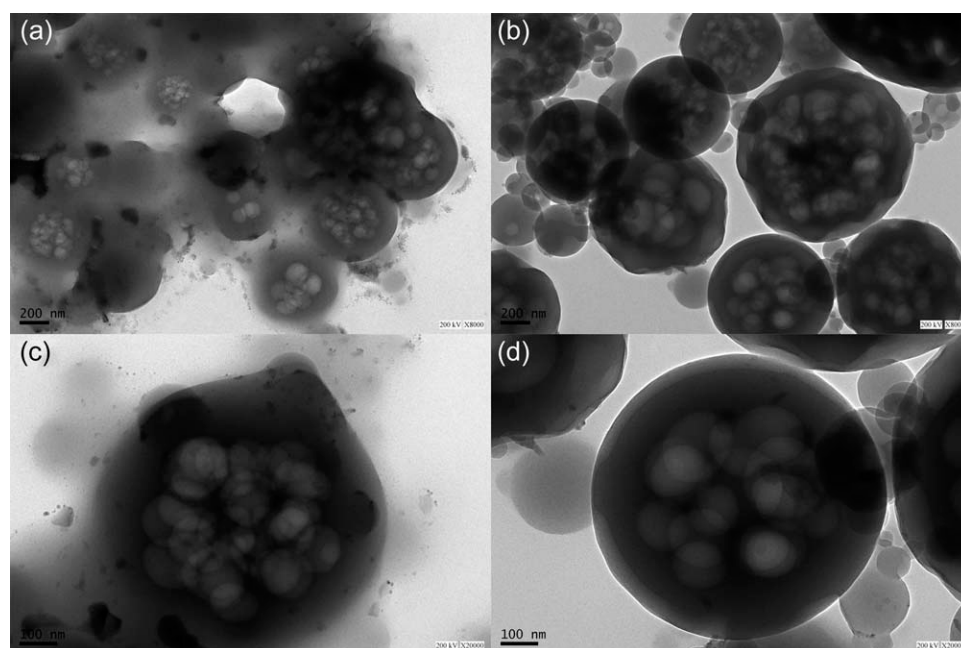


**Figure 3** TEM images of samples with different initiator: (a), (c) KPS in Run 2 and (b), and (d) AIBN in Run 3.

nanocapsules coexist with a mass of small pure PSt spheres in the system with 0.3 wt % DDT in Run 4 [Fig. 4(b,d)]. This can also be proved by the difference in the size distribution curves, as shown in Figure 2(c,d). In Figure 2(c), when AIBN is used, the particle size distribution is monomodal: most of particles were nanocapsules. In Figure 2(d), the particle size distribution becomes bimodal: nanoparticles with smaller size and nanocapsules with larger size. The

undesirable nanoparticles can be easily ascribed to homogenous nucleation. Homogenous nucleation could be partially suppressed by the replace of DDT with DVB content as indicated by the corresponding decrease of the amount of small solid particles from Figure 4(b) to Figure 4(a). This can be ascribed to the formation of the crosslinked shell suppressing the radical exit from the particles to the aqueous phase and thus polymerization in the aqueous phase.<sup>21</sup>

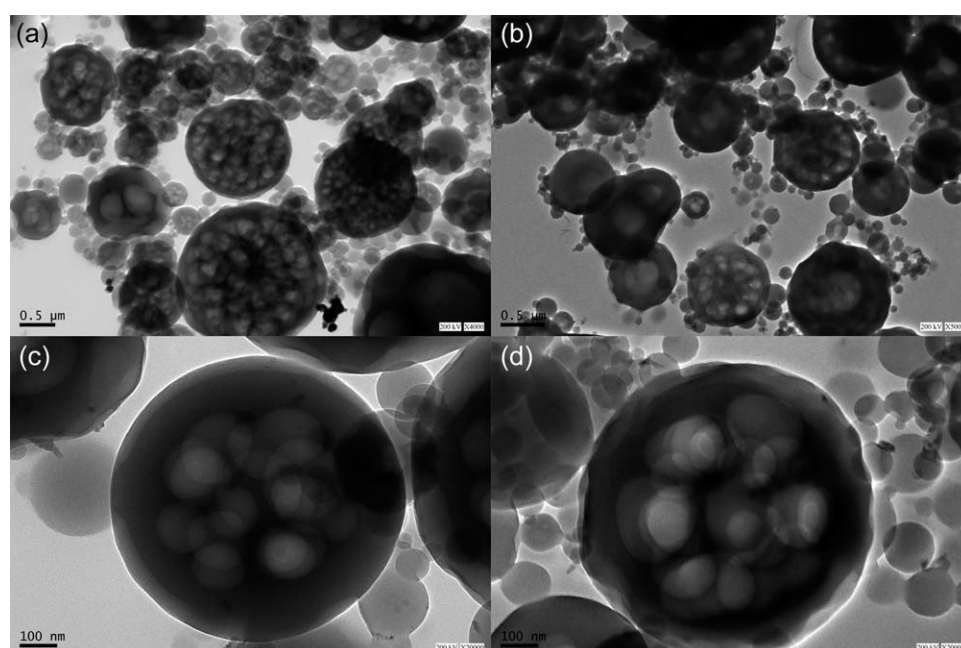


**Figure 4** TEM images of samples with crosslinking agents DVB and chain-transfer agent DDT: (a), (c) 1% DVB in Run 3 and (b), and (d) 0.3% DDT in Run 4.

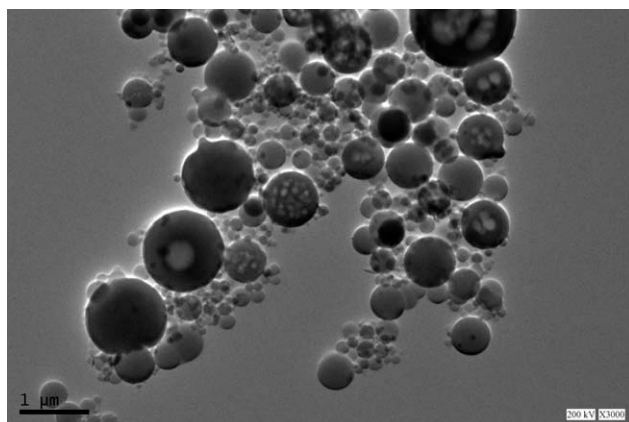


**Figure 5** TEM image of sample with 1.5 wt % DNS-86 in Run 5.

For Figure 4(c), 1.0 wt % DVB was used, and the morphology suggests that the shell of nanocapsule is thick and stable. In Figure 4(d), with 0.3 wt % DDT replacing DVB, the particle presents a thin and distorted shell. In the presence of DDT, a chain-transfer agent, the polymer (PSt) chains are shorter, which lead to a thin and distorted shell. For the systems with DVB, cross-linker, a network was created between the polymer (PSt) chains, which would covalently hold the polymer shell to be an integrity to enhance the stability of nanocapsules.

Whatever DVB or DDT was used in this system, the mobility of polymer chains is enough for phase separation. It is apparent that as the DDT was used, the molecular weight decreases, the particles become more irregular, and only a small fraction of nanocapsules was created. When DVB was used, the particles have greater uniformity, and nanocapsules dominated in the latex particles.

### Influence of the surfactant type

It is well known that the stability of miniemulsions is to a large extent determined by the interfacial properties of the participating phases and can be optimized by the use of a suitable surfactant that lowers the interfacial tension to against coalescence. Hence, we change the type of surfactant added into the system to investigate different surfactants' effect on the morphology of latex particle.

Figure 5 shows a TEM image for 1.5 wt % DNS-86 in Run 5. Most of the particles do not contain CP. A limited number of the larger nanocapsules are created as seen in the image. For Figure 4(a) in Run 3, the surfactant system was composed of 1.0 wt % nonionic surfactant OP-10 and 0.5 wt % SDS. In contrast to Figure 5, the TEM image shows that nearly all latex particles are nanocapsules. It is possible that the combination of ionic and nonionic surfactants

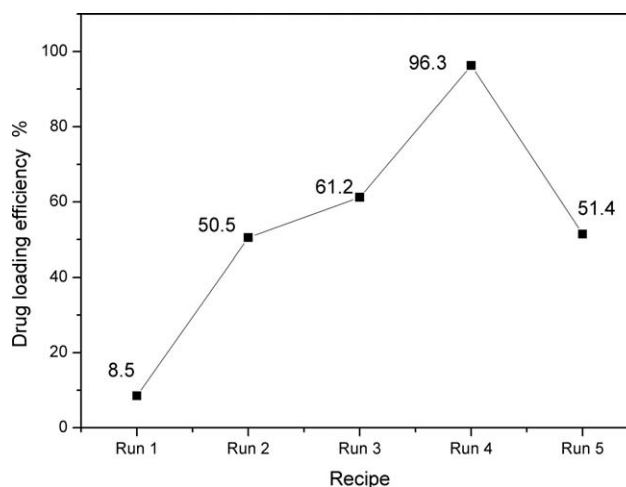


**Figure 6** Drug-loading efficiency of different recipe.

could improve the morphology of capsules and lead to a large fraction of nanocapsules.

### Drug-loading efficiency of nanocapsules

The drug-loading efficiency of CP in nanocapsules is affected significantly by increasing the amount of CP. As shown in Figure 6, the drug-loading efficiency linearly increased from 8.5 to 50.5% when the amount of CP was increased from 3.3 to 10 g. Replacing initiator KPS with DVB led to an increase of drug-loading efficiency from 50.5 to 61.2%. As mentioned earlier, this may be because of the usage of the hydrophobic initiator AIBN, facilitating the encapsulation of CP in our case.

Interestingly, we found that the drug-loading efficiency of run 4 is incredibly high, 96.3% here. This result may be explained by the fact that through the addition of a chain-transfer agent (DDT), the molecular weight of the polymer decreases, the PSt chains are so short that it dissolved into acetone. In the process of Soxhlet extracting, the PSt chains are extracting with CP together by acetone, which led to the high-drug-loading efficiency. When 1.5 wt % DNS-86 is used in Run 5, the drug-loading efficiency is 51.4%, which is lower than that of Run 3.

### Properties of the nanocapsules

As case study, the properties of the nanocapsules of run 3 were fully characterized by FTIR,  $^1\text{H-NMR}$ , and DSC measurements.

The FTIR spectra of pure CP (a), nanocapsules (b), and the PSt (c) are shown in Figure 7. It is found that the adsorption of CP at 486, 693, and 881  $\text{cm}^{-1}$  appeared in the spectrum of the nanocapsules, while after Soxhlet extraction, those peaks of adsorption are disappeared in Figure 7(c). The peak marked with (a), (b), (c), (d), and (e) in the  $^1\text{H-NMR}$

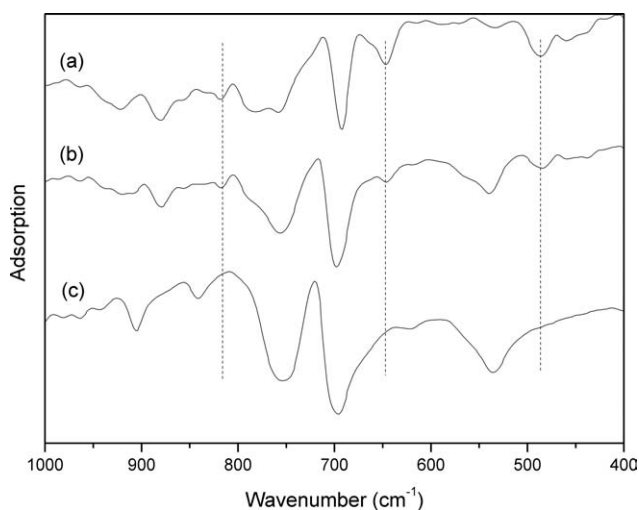


**Figure 7** FTIR spectra of pure CP (a), nanocapsule (b), and PSt (c).

spectrum is attributable to the correspondence groups in the chemical structure of CP, as shown in Figure 8. After Soxhlet extraction, those peaks are also disappeared, and just signal peaks of PSt are left. Thus, both the FTIR and  $^1\text{H-NMR}$  spectra indicated that CP had been loaded into the nanocapsules.

DSC is also performed to analyze the nature of the nanocapsules. The DSC curves of pure CP (a), nanocapsules (b), and the PSt (c) are shown in Figure 9. As shown in Figure 9(a), the pure CP melting point is  $-33.1^\circ\text{C}$ , and the melting peak is sharp. In Figure 9(b), the CP melting peak was also found in DSC measurement of the nanocapsules, but the peak is broad, and the melting point is higher than that of

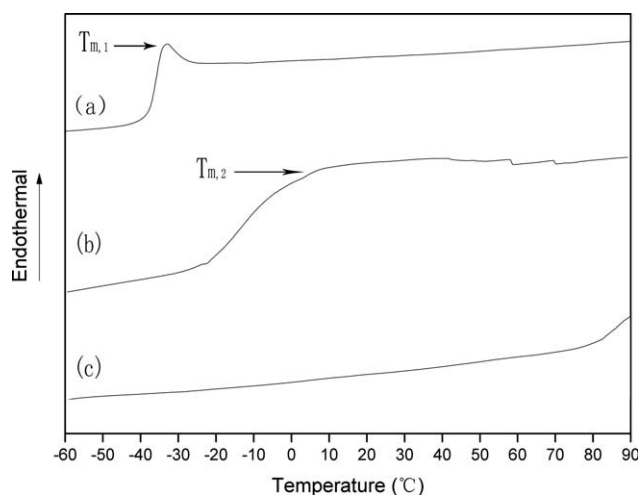


**Figure 9** DSC curve of pure CP (a), nanocapsule (b), and PSt (c).

pure CP. This result may be explained by the fact that the CP is encapsulated in the nanocapsules, and the shell of nanocapsule affects thermodynamic behavior of CP encapsulated in nanocapsules. After Soxhlet extraction, no CP melting peak was found in DSC measurement of the PSt, indicating that the core materials (CP) were completely removed.

## CONCLUSIONS

Nanocapsules containing CP encapsulated with a PSt shell were synthesized by means of miniemulsion polymerization. The effects of conditions, including the type of the surfactant, initiator, the monomer/CP ratio, and the level of the crosslinking

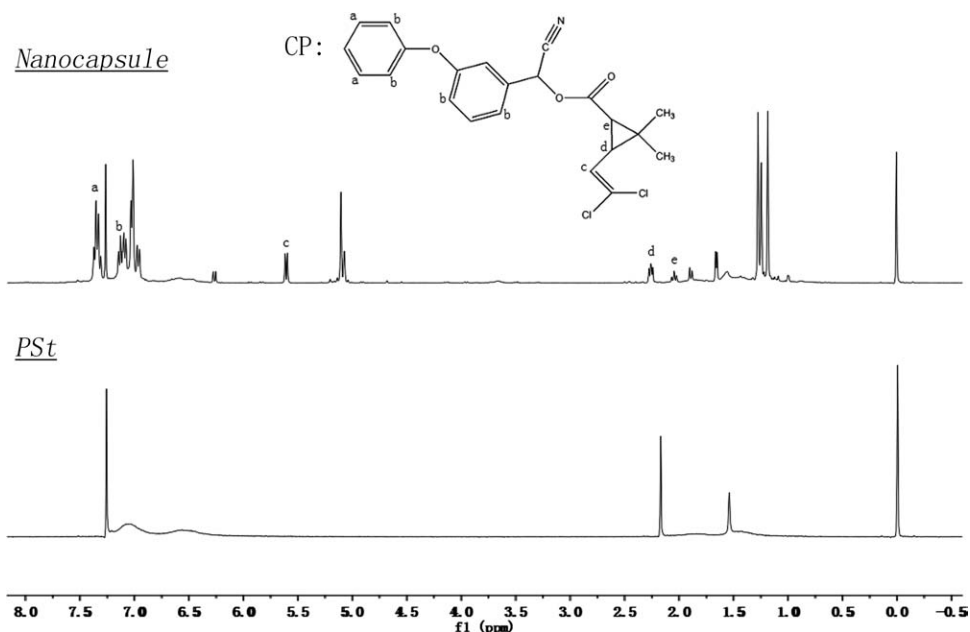


**Figure 8**  $^1\text{H}$  NMR spectra of nanocapsule (a) and PSt (b) recorded in  $\text{CDCl}_3$

agent or chain-transfer agent were investigated. A large content of monomer in the oil phase is detrimental to the formation of nanocapsules. The oil-soluble initiator AIBN is advised to be used in our case, facilitating the encapsulation of CP. DDT is not advised to be introduced into studied system, because it can lead to a shorter polymer chain that make shell of nanocapsules thin and distorted. The combination of ionic and nonionic surfactants could improve the morphology of capsules and lead to a large fraction of nanocapsules. About 1.0 wt % SDS, 0.5 wt % OP-10, 1.0 wt % AIBN, and 1.0 wt % DVB of recipe in Run 3 were optimum levels for obtaining well-defined nanocapsules of CP with a St/CP ratio of 1 : 1.

## References

1. Putlitz, B. Z.; Landfester, K.; Fischer, H.; Antonietti, M. *Adv Mater* 2001, 13, 500.
2. Tissot, I.; Novat, C.; Lefebvre, F.; Bourgeat-Lami, E. *Macromolecules* 2001, 34, 5737.
3. Chen, M.; Wu, L.; Zhou, S.; You, B. *Adv Mater* 2006, 18, 801.
4. Mandal, T. K.; Fleming, M. S.; Walt, D. R. *Chem Mater* 2000, 12, 3481.
5. Caruso, F.; Caruso, R. A.; Mhwald, H. *Science* 1998, 282, 1111.
6. Donath, E.; Sukhorukov, G. B.; Caruso, F.; Davis, S. A.; Möhwald, H. *Angew Chem Int Ed* 1998, 37, 2201.
7. Gao, C.; Leporatti, S.; Moya, S.; Donath, E.; Mhwald, H. *Langmuir* 2001, 17, 3491.
8. Sukhorukov, G. B.; Donath, E.; Davis, S.; Lichtenfeld, H.; Caruso, F.; Popov, V. I.; Möhwald, H. *Polym Adv Technol* 1998, 9, 759.
9. Jang, J.; Bae, J. *Chem Commun* 2005, 1200.
10. Tiarks, F.; Landfester, K.; Antonietti, M. *Langmuir* 2001, 17, 908.
11. Luo, Y.; Gu, H. *Macromol Rapid Commun* 2006, 27, 21.
12. McDonald, C. J.; Bouck, K. J.; Chaput, A. B.; Stevens, C. J. *Macromolecules* 2000, 33, 1593.
13. Ni, K.-F.; Shan, G.-R.; Weng, Z.-X. *Macromolecules* 2006, 39, 2529.
14. van Zyl, A. J. P.; Sanderson, R. D.; de Wet-Roos, D.; Klumperman, B. *Macromolecules* 2003, 36, 8621.
15. Landfester, K. *Angew Chem Int Ed* 2009, 48, 4488.
16. Dowd, P. F.; Gagne, C. C.; Sparks, T. C. *Pest Biochem Physiol* 1987, 28, 9.
17. Stephenson, R. R. *Aquat Toxicol* 1982, 2, 175.
18. Cao, Z. H.; Shan, G. R.; Sheibat-Othman, N.; Putaux, J. L.; Bourgeat-Lami, E. *J Polym Sci Part A: Polym Chem* 2010, 48, 593.
19. Luo, Y.; Zhou, X. *J Polym Sci Part A: Polym Chem* 2004, 42, 2145.
20. Chern, C.-S.; Liou, Y.-C. *J Polym Sci Part A: Polym Chem* 1999, 37, 2537.
21. Cao, Z.; Schrade, A.; Landfester, K.; Ziener, U. *J Polym Sci Part A: Polym Chem* 2011, 49, 2382.